 © 2007 The Chemical Society of Japan

π-Radical Cationic Salts of Tetrathiafulvalene Derivatives with Pyromellitate

Kazuhiko Shiono, Toshio Naito, and Tamotsu Inabe*

Division of Chemistry, Graduate School of Science, Hokkaido University, Sapporo 060-0810

Received July 31, 2006; E-mail: inabe@sci.hokudai.ac.jp

Pyromellitate is known to form hydrogen-bonding anionic networks when the number of deprotonation from pyromellitic acid is one or two. This unique anion has been utilized for the construction of the π-radical cationic salts of the tetrathiafulvalene (TTF) derivatives. In the crystals of three kinds of the TTF salts and the tetramethyltetraselenafulvalene salt, pyromellitate was found to form two-dimensional sheets. The anions in the two TTF salts were connected by rhombic-type inter-anionic connection, which is a typical inter-anionic connection pattern for pyromellitate. The TTF derivatives were all in a π-radical mono-cationic state and dimerized in a space dictated by the anionic networks. The extra space in the crystals was filled with crystal solvents. On the other hand, in the crystals of the ethylenedithia-tetrathiafulvalene salts, pyromellitate formed only intra-molecular hydrogen bonds. The anion was thus isolated in these crystals.

Hydrogen bonds are a very powerful tool to regulate molecular arrangement and utilized frequently in crystal engineering for the design of second harmonic generation (SHG) active crystals. Electronic functionalities, such as electrical conduction and magnetic properties, also depend strongly on intermolecular interactions; thus, regulation of the molecular arrangement is also important for the design of conductors and magnets. Recent approaches, therefore, include crystal engineering for molecular design, and in most of the cases, functional groups are directly attached to the component itself. On the other hand, our approach is based on the formation of networks of the counter ions; when one of the components in a two-component crystal has hydrogen-bonding functional groups and forms networks, the counter component may be packed in/between the networks. From this point of view, we have examined network formation of mellitate, which is the deprotonated anion of benzenehexacarboxylic acid (mellitic acid; Scheme 1).[1–3] It has been found that the anion forms self-organized networks, since strong hydrogen bonds between carboxy and carboxylato groups occur between the anions. Counter cationic components, thus, cannot spontaneously assemble, and unique arrangements are imposed by the network conformations. This methodology, indeed, has afforded unique structures, such as a helical one-dimensional tetrathiafulvalene (TTF) column[4,5] and a coplanar tetramethyltetrathiafulvalene (TMTTF) two-dimensional sheet.[5]

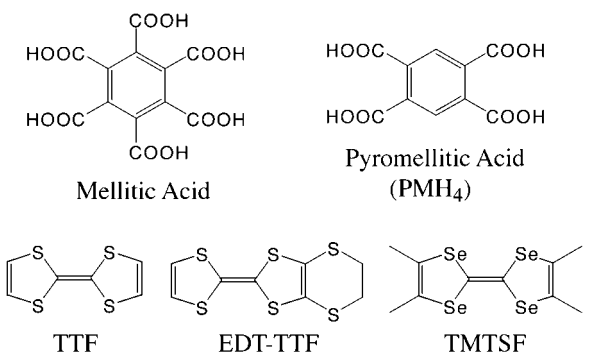

Scheme 1.

Pyromellitate is an anionic species of a member of benzenepolycarboxylic acid family. Similar to mellitate, this anion is expected to form anionic networks, and the structural investigations have already been performed for salts with organic ammonium cationic species by several research groups.[6–10] Herein, we use the abbreviation of PMH_4 for pyromellitic acid (Scheme 1), and the anion is then described as $(PMH_{4-n})^{n-}$, where n is deprotonation number. So far, the structures of the salts with $n = 1$ and 2 have been studied, and the network structures found are summarized in Fig. 1 (networks bridged by solvents are omitted). The most notable difference from those of mellitate lies in the ability of intra-molecular hydrogen bonds in $(PMH_{4-n})^{n-}$. Since lack of substituents at 3- and 6-positions allows the neighboring carboxy and carboxylate groups to be co-planar, a proton-sharing intra-molecular hydrogen-bond forms (Fig. 1(iii)). The two-dimensional (2-D) sheet-like networks are known for the anion with $n = 1$; the network in Fig. 1a has been observed for imidazolium[6] and pyridinium[7] salts, and that in (b) has been found for a 4-(dimethylamino)pyridinium salt.[8] For the anion with $n = 2$, Zaworotko and Biradha have reported that the anion arrangement varies from 0-D (Fig. 1c), in which hydrogen bonds occur only within a single anion, to the networks with 1-D (Fig. 1d), 2-D (Fig. 1f), and 3-D (Fig. 1g).[9] A different type of the 1-D network (Fig. 1e) has been found for 1,7-phenanthrolinium[8] and cyclic diamidinium[10] salts. The 1-D chain in (e) is the same as the 1-D mellitate network,[2] and 2-D sheets of (a) and (f) are similar to that in the 2-D mellitate network which is made of rhombic hydrogen bonds.[3] In addition, the 2-D sheet in (b) is analogous to this rhombic-type network. From these facts, we think that $(PMH_{4-n})^{n-}$ is a promising candidate for forming networks. We have examined how the

Published on the web March 13, 2007; doi:10.1246/bcsj.80.476

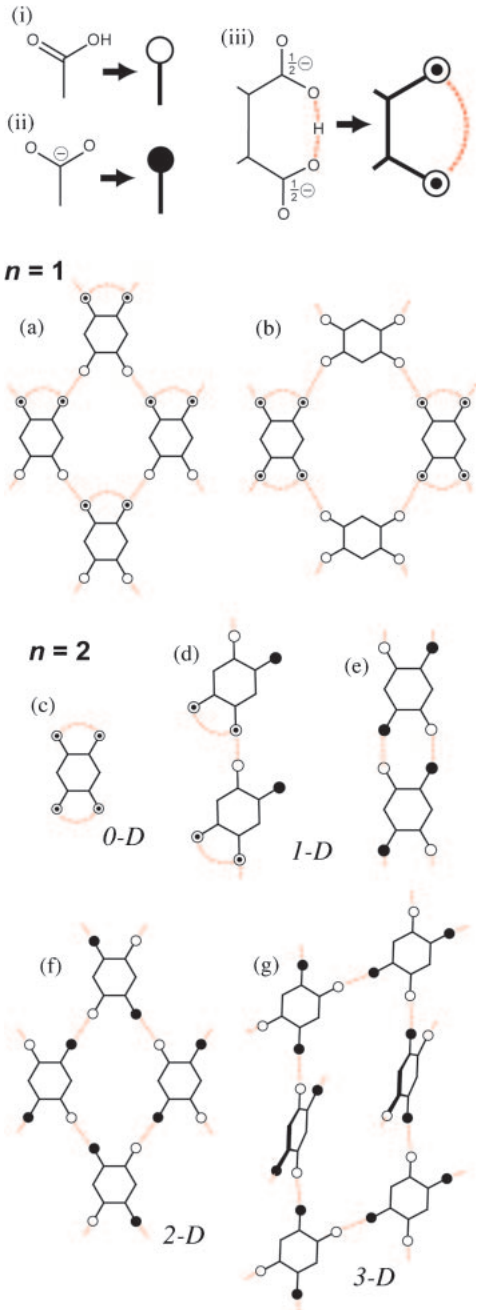

Fig. 1. Schematic representation of carboxy and carboxylato groups (i)–(iii), and network types found in various organic cationic salts of pyromellitate for $n = 1$ (a) and (b), and for $n = 2$ (c)–(g). Hydrogen bonds are shown by red dotted lines.

anionic networks affect the arrangement of the cations.

The cationic components selected were π-radical cations of the TTF family. These have an open-shell π-orbital that becomes a source of the electronic functionality, while they have strong tendency to be self-assembled due to the attractive interactions operating through overlapping open-shell orbitals. In the mellitate salts, the self-assembling ability of the anion exceeds that of the TTF cations to some extent, resulting in the suppression of the π–π interactions between the cations.[4,5] On the other hand, the decreased number of the hydrogen-bonding functional groups in pyromellitate is expected to affect the energy of network formation. The weaker assembling ability of pyromellitate compared with mellitate should be reflected in the resultant structures.

In this paper, we describe the crystal structures and hydrogen-bonding networks in the six pyromellitate salt crystals obtained by electrochemical crystal growth using TTF, ethylenedithia-tetrathiafulvalene (EDT-TTF), and tetramethyltetraselenafulvalene (TMTSF) (Scheme 1).

Experimental

Materials. The following three methods were used to prepare the crystalline products.

Method A: Pyromellitic acid (50 mg) was first dissolved in methanol (5–25 mL) in an electrochemical cell, and dichloromethane (20–25 mL) was added for a total amount 35–45 mL. Then, the donor (10 mg) and pyridine or 4-*t*-butylpyridine (molar ratio to pyromellitic acid was 10:1) was added to the solution. A constant current of 9 µA was applied to the cell, which gave crystals in a few days.

Method B: Potassium salts of pyromellitate were prepared by acid–base reaction for $n = 1$ and 2, respectively. The salt (20 mg) was dissolved in methanol (10–15 mL) in an electrochemical cell, and then dichloromethane (25–30 mL) and the donor (10 mg) were added. A constant current of 9 µA was applied to the cell, which gave crystals in a few days.

Method C: Pyromellitic acid (20 mg) and trimesic acid (20 mg) were dissolved in methanol (15–20 mL) in an electrochemical cell, and dichloromethane (25 mL) was added. Then, the donor (10 mg) and pyridine (molar ratio to the acid was 10:1) was added to the solution. A constant current of 9 µA was applied to the cell, which gave crystals in a few days.

The crystals obtained were $[TTF^+][(PMH_3)^-]\cdot CH_2Cl_2$ (**1**: Methods A and B), $[TTF^+]_2[(PMH_2)^{2-}]\cdot H_2O$ (**2**: Method B), $[TTF^+]_2[(PMH_2)^{2-}]\cdot CH_2Cl_2$ (**3**: Method C), α-$[EDT\text{-}TTF^+]_2$-$[(PMH_2)^{2-}]$ (**4**: Method A), β-$[EDT\text{-}TTF^+]_2[(PMH_2)^{2-}]$ (**5**: Method C), and $[TMTSF^+]_2[(PMH_2)^{2-}](PMH_4)\cdot 2CH_2Cl_2$ (**6**: Method A). Though **4** and **5** have the same composition, they are different as shown later.

X-ray Structure Analyses. Diffraction data were recorded on a Rigaku R-AXIS Rapid imaging plate diffractometer with graphite-monochromated Mo Kα radiation ($\lambda = 0.7107$ Å). The crystal data are summarized in Table 1. The structures were solved using direct methods (SIR-92[11] or SHELX97[12]) and refined with all data on F^2 using the CrystalStructure program package.[13] Full-matrix least-squares refinements were performed for non-hydrogen atoms with anisotropic thermal parameters, except for the crystal solvent in **1** (isotropic).

The hydrogen positions in the O–H···O hydrogen-bonds were determined by applying the geometrical features as follows.[2] The deprotonation from a carboxy group was determined from the ratio ($r = a/b$) of lengths of the two C–O bonds (a and b; $a \geq b$) in a single carboxy/carboxylato group. An r value larger than 1.07 with an O–H···O hydrogen-bond distance between two carboxy/carboxylato groups longer than about 2.5 Å is characteristic of a carboxy group. Deprotonation occurred in a species with an r value smaller than 1.03 and an O···O distance between two carboxy/carboxylato groups longer than about 2.5 Å. When $1.03 < r < 1.07$ and the hydrogen-bond distance between two carboxy/carboxylato groups was very short (O···O < 2.5 Å), the proton was thought to be equally shared by the two oxygen atoms

Table 1. Crystal Data and Structural Refinement Parameters

Compound	**1**	**2**	**3**	**4**	**5**	**6**
Formula	$C_{17}H_{11}Cl_2O_8S_4$	$C_{22}H_{16}O_{10}S_8$	$C_{23}H_{14}Cl_2O_8S_8$	$C_{26}H_{16}O_8S_{12}$	$C_{22}H_{16}O_8S_{12}$	$C_{42}H_{38}Cl_4O_{16}Se_8$
Formula weight	542.42	696.84	745.74	841.13	793.08	1572.24
Crystal system	triclinic	triclinic	orthorhombic	triclinic	monoclinic	triclinic
Space group	$P\bar{1}$	$P\bar{1}$	$Cmc2_1$	$P\bar{1}$	$C2/c$	$P\bar{1}$
a/Å	9.807(3)	7.26(1)	15.813(6)	9.306(2)	12.517(6)	7.475(4)
b/Å	9.798(2)	10.08(1)	28.17(1)	9.507(2)	36.61(1)	10.378(4)
c/Å	11.781(2)	10.75(1)	12.933(4)	9.942(2)	7.659(3)	16.888(9)
α/°	84.45(1)	108.95(8)	—	114.44(1)	—	77.33(4)
β/°	73.28(2)	106.48(5)	—	99.28(1)	120.27	88.46(5)
γ/°	87.47(1)	104.73(5)	—	98.27(1)	—	76.22(4)
V/Å^3	1078.9(4)	659(1)	5761(3)	768.2(3)	3031(2)	1240(1)
Z	2	1	8	1	4	1
D_{calcd}/g cm^{-3}	1.670	1.755	1.719	1.818	1.737	2.104
μ(Mo Kα)/cm^{-1}	7.31	7.34	8.53	9.05	9.11	61.75
Temp. of data collection/K	296	123	123	123	123	123
No. of unique reflections	4876	3006	6830	3488	3480	5292
R_{int}	0.030	0.024	0.044	0.030	0.047	0.048
No. of variables	276	189	404	216	224	335
$R1$ [$I > 2.0\sigma(I)$]	0.078	0.036	0.039	0.040	0.091	0.058
R, R_w (F^2, all data)	0.091, 0.233	0.056, 0.098	0.047, 0.094	0.069, 0.088	0.106, 0.232	0.071, 0.144
GOF indicator	1.916	1.019	1.011	1.092	1.451	1.443

Table 2. C–O Bond Lengths and r in Pyromellitate Anions

	Carboxy (carboxylato) group	a/Å	b/Å	r
1	A	1.270(5)	1.215(4)	1.05
	B	1.269(5)	1.219(4)	1.04
	C	1.307(5)	1.208(6)	1.08
	D	1.286(5)	1.208(6)	1.06
2	A	1.264(3)	1.234(3)	1.02
	B	1.312(3)	1.210(2)	1.08
3	A	1.275(4)	1.208(4)	1.06
	B	1.267(3)	1.207(3)	1.05
	C	1.287(3)	1.208(3)	1.07
	D	1.277(3)	1.212(3)	1.05
4	A	1.256(4)	1.225(5)	1.03
	B	1.271(3)	1.208(5)	1.05
5	A	1.280(8)	1.221(6)	1.05
	B	1.290(8)	1.227(6)	1.05
6	A	1.287(8)	1.240(7)	1.04
	B	1.318(9)	1.212(9)	1.09
	C	1.308(6)	1.223(8)	1.07
	D	1.317(6)	1.223(6)	1.08

Table 3. Selected Hydrogen-Bonds between Carboxy/Carboxylato Groups or with Water Molecules

	Groups	O···O distance/Å	Symmetry operation
1	A···B	2.374(4)	
	A···C^{i}	2.650(4)	$x, y+1, z$
	B···D^{ii}	2.645(4)	$x+1, y, z$
2	A···O$_w$	2.771(3)	
	A···O$_w$^{i}	2.761(2)	$-x+1, -y, -z+2$
	B···O$_w$^{ii}	2.596(3)	$x, y, z-1$
3	A···B^{i}	2.435(3)	$-x+1/2, -y+3/2, z+1/2$
	C···D^{ii}	2.435(3)	$x, -y+1, z-1/2$
4	A···B	2.387(5)	
5	A···B	2.373(5)	
6	A···C	2.483(7)	
	A^{i}···D	2.603(6)	$x-1, y, z$
	A···B^{ii}	2.879(4)	$-x+1, -y+1, -z+2$

of the different carboxy/carboxylato groups (deprotonation number is 0.5). The atom to which the hydrogen was attached was determined from the geometrical features, and the position was finally determined by the difference Fourier maps (**1**, **2**, **4**, and **5**) or assigned at an ideal position (**3** and **6**) due to broad electron density peaks (fixed position with isotropic thermal parameters). The other hydrogen atoms were placed at the ideal positions and included in the refinement with a riding model.

Crystallographic data have been deposited with Cambridge Crystallographic Data Centre: Deposition numbers CCDC 624753-624758 for compounds **1** to **6**. Copies of the data can be obtained free of charge via http://www.ccdc.cam.ac.uk/conts/retrieving.html (or from the Cambridge Crystallographic Data Centre, 12, Union Road, Cambridge, CB2 1EZ, UK; Fax: +44 1223 336033; e-mail: deposit@ccdc.cam.ac.uk).

Results and Discussion

The charge on each component in the crystal was mainly determined from n. The r values of the carboxy/carboxylato groups for the determination of n are summarized in Table 2. The O···O distances in the hydrogen bonds found in these crystals are listed in Table 3.

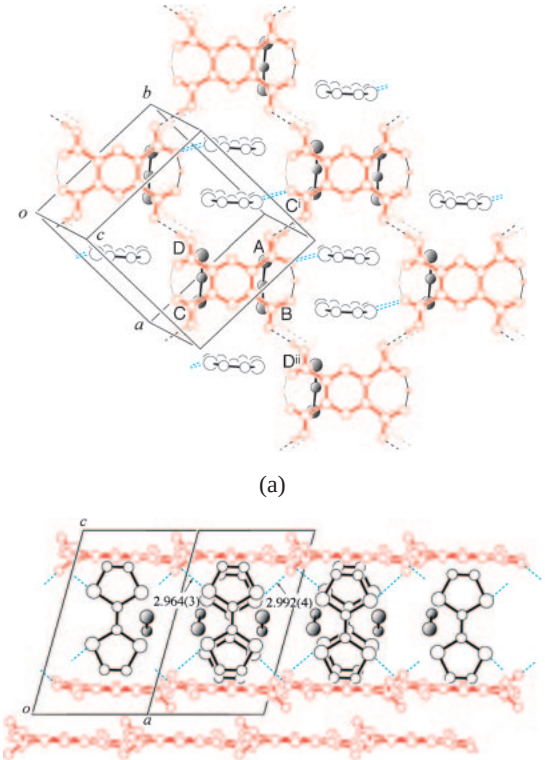

(a)

(b)

Fig. 2. Molecular arrangement in the TTF salt **1**. View perpendicular to the 2-D anionic sheet (a) and view parallel to the sheet (b). Pyromellitate is shown in red, hydrogen bonds are in black broken or solid lines, and short S···O contacts are in blue dotted lines. Gray spheres are CH_2Cl_2. Lightly colored moieties in (a) are pyromellitate located behind the TTF and CH_2Cl_2 moieties. Hydrogen atoms not involved in hydrogen bonds are omitted.

$[TTF^+][(PMH_3)^-]\cdot CH_2Cl_2$ (1). The geometries of four independent carboxy/carboxylato groups (A to D in Fig. 2a) are summarized in Table 2. The *r* values of A and B suggest that both are in the intermediate region. Indeed, a hydrogen bond with an extremely short O···O distance has formed between A and B; one proton is shared by the two oxygen atoms in A and B. The large *r* value clearly indicates that C is a carboxy group. On the other hand, the *r* value of D is in the intermediate region. However, this group is assigned as a carboxy group since a hydrogen bond is present between D and one of the oxygen atoms in B, which does not have proton (Fig. 2a and Table 3). If both C and D are carboxy groups, there is no possibility of the intra-molecular hydrogen bond. Indeed, the shortest O···O contact (2.960(5) Å) between C and D is nearly twice of the van der Waals radius of oxygen (1.5 Å), which is significantly longer than the ordinary O···O distance in the intra-molecular hydrogen bond. Consequently, *n* equals 1 for each anion, and the charge on TTF is thus +1. The bond lengths sensitive to the charge on the TTF framework are compiled in Table 4. The geometrical features of TTF are consistent with its mono-cation radical.

In the crystal, $(PMH_3)^-$ has a 2-D sheet-like network parallel to the *ab* plane through A···C and B···D hydrogen bonds, as shown in Fig. 2a. This network is the same as the rhombic-type network shown in Fig. 1a. The large void in the network is filled by the CH=CH terminal moieties of the dimerized TTFs.

Table 4. Bond Lengths in the TTF Framework (Averaged under the Assumption of D_{2h} Point Group Symmetry)

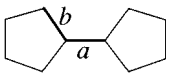

Compound	a/Å	b/Å	Reference
1	1.407	1.723	
2	1.395	1.720	
3	1.389 1.384 1.390 1.368	1.708 1.711 1.710 1.719	
TTF^0	1.349	1.757	14
$[TTF^+][Br^-]$	1.393	1.720	15
4	1.393	1.713	
5	1.26 1.38	1.77 1.73	
$EDT\text{-}TTF^0$	1.335	1.758	16
$[EDT\text{-}TTF^+][I_3^-]$	1.40	1.716	17
6	1.385	1.865	
$TMTSF^0$	1.352	1.892	18
$[TMTSF^+][ReO_4^-](C_2H_3Cl_3)_{0.25}$	1.41	1.86	19

Molecular packing between the anionic sheets is shown in Fig. 2b. The rather large space between the TTF dimers is filled with CH_2Cl_2 molecules, and the dimer is completely isolated. There are fairly short S···O contacts between the TTF cation and the anions. As a result, a 2-D extended sandwich-type layer unit is composed of (anionic sheet)···(TTF radical cation dimers + CH_2Cl_2)···(anionic sheet), which stacks along the *c* axis in the crystal.

$[TTF^+]_2[(PMH_2)^{2-}]\cdot H_2O$ (2). The *r* values of the two independent carboxy/carboxylato groups (Fig. 3a and Table 2) indicate that A is a carboxy group and B is a carboxylato group. Since the anion is located on an inversion center, *n* has to be 2. TTF is in a π-radical mono-cationic state from the composition, and this is consistent with the geometrical feature of TTF (Table 4).

As shown in Fig. 3a, $(PMH_2)^{2-}$ is arranged in a 2-D sheet. However, there are no direct inter-anionic hydrogen bonds between them; they are all connected through hydrogen bonds mediated by H_2O molecules. Nevertheless, the anionic sheet is rather condense, and additional C–H···O hydrogen bonds with a relatively short C···O distance (3.197(3) Å) between the anions can be noted.

The TTFs sandwiched between these sheets form a 1-D column along the *a* axis (Figs. 3b and 3c). The two-fold stacking periodicity in the column coincides with the repeat unit of the anionic sheet along the *a* axis. The S···O contacts are rather short, and this causes the two-fold periodicity.

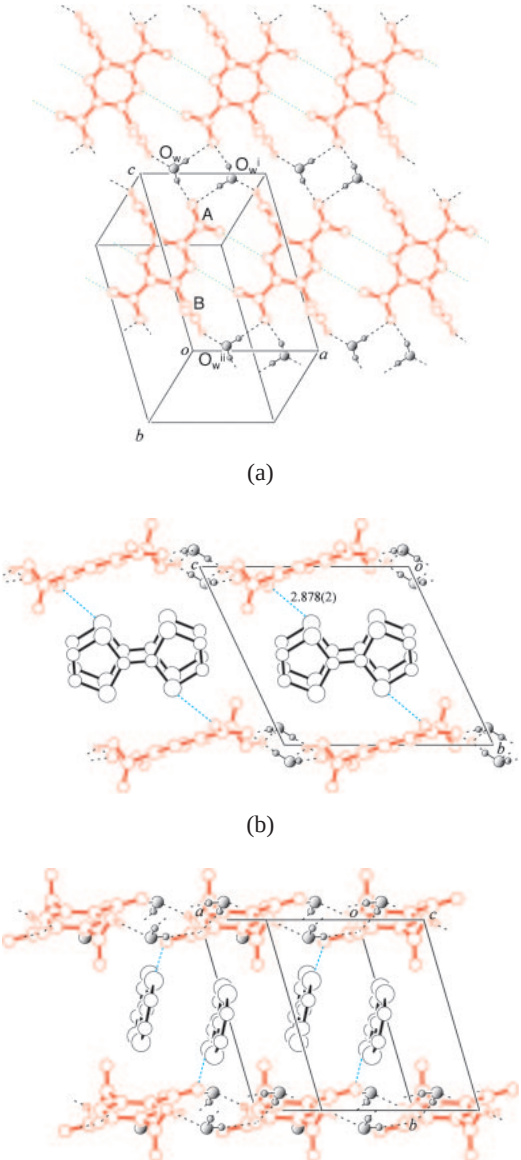

(a)

(b)

(c)

Fig. 3. Molecular arrangement in the TTF salt **2**. View perpendicular to the 2-D anionic sheet (a), view parallel to both the sheet and the TTF column (b), and view parallel to the sheet but perpendicular to the TTF column (c). Gray spheres are H_2O. Hydrogen atoms not involved in hydrogen bonds are omitted. Green dotted lines in (a) are C–H···O short contacts.

$[TTF^+]_2[(PMH_2)^{2-}]\cdot CH_2Cl_2$ (3). The geometries of the independent four carboxy/carboxylato groups (A to D in Fig. 4a) are summarized in Table 2. All of the r values are around the boundary between intermediate and carboxy regions. In addition, there are only two kinds of hydrogen bonds between the anions (A···B and C···D), and both of them are quite short (Table 3). On the basis of the hydrogen-bonding network pattern in Fig. 4a, all four groups appear to have a value of n of 0.5, though the protons are not located exactly at the midpoint of each hydrogen bond. The possibility of any intra-molecular hydrogen bond has been ruled out, since

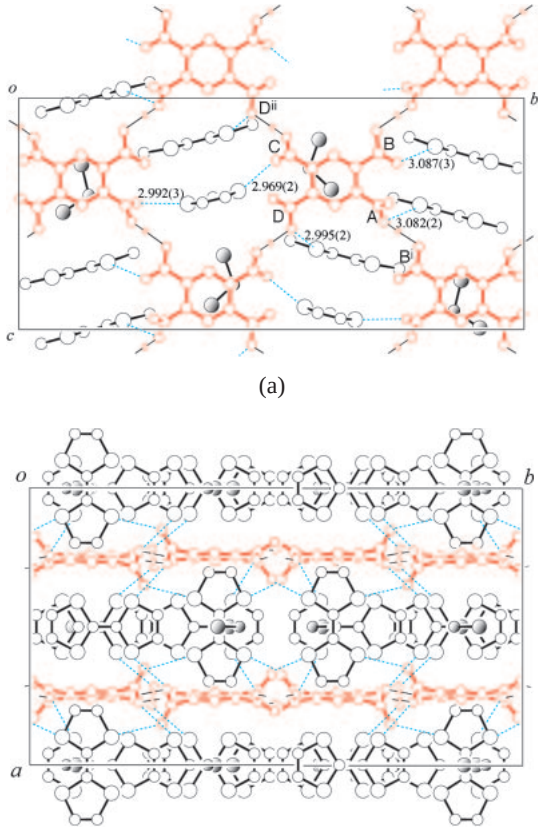

(a)

(b)

Fig. 4. Molecular arrangement in the TTF salt **3**. View perpendicular to the 2-D anionic sheet (a) and view parallel to the sheet (b). Gray spheres are CH_2Cl_2. Hydrogen atoms not involved in hydrogen bonds are omitted.

the shortest O···O contact within the anion exceeds 3 Å. The n value is therefore 2, and all of the TTFs are in a π-radical mono-cationic state. As shown in Table 4, the geometrical features of TTF are consistent with this assignment.

The anionic arrangement in Fig. 4a may correspond to the rhombic-type network shown in Fig. 1f, and is very similar to that in **1**. The inter-anionic hydrogen bonds are shorter in **3** than in **1**, and the void size is relatively smaller in **3** (one of the diagonals of the rhombic hole linked by the unsubstituted CH portions of the anions is 10.817 Å in **1** and 10.213 Å in **3** (in C···C distance)). In **1**, two terminal CH=CH moieties of the TTF dimer fit into this rhombic hole, whereas only one terminal CH=CH moiety is inserted into this hole in **3** (Fig. 4b). The TTF cation with its long axis perpendicular to the anionic plane has several short S···O contacts with the anions, and the orientation and position are completely fixed. Therefore, there is not enough space to form an eclipsed-type face-to-face stacked dimer, resulting in a cross-shaped dimer. Such criss-cross π–π interaction has also been observed for $[TTF]_3(M_6O_{19})$ (M = Mo and W).[20] In the crystal, there is another type of the TTF dimer; eclipsed-type face-to-face stacked dimer with their long axes parallel to the anionic sheet. Every space between these dimers is filled with CH_2Cl_2, and the dimers are consequently isolated.

α-$[EDT\text{-}TTF^+]_2[(PMH_2)^{2-}]$ (4). The r values of two in-

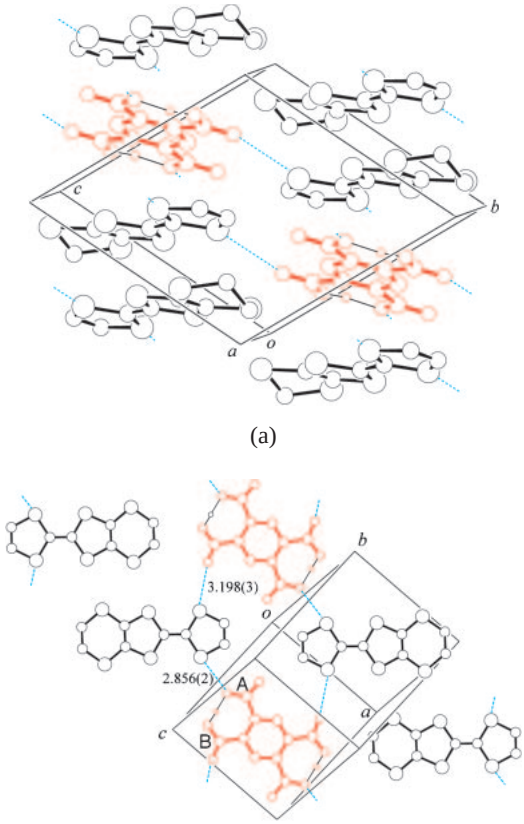

Fig. 5. Molecular arrangement in the EDT-TTF salt **4**. Structure of the mixed-stacked column (a) and view perpendicular to the anionic plane (b).

dependent carboxy/carboxylato groups (A and B in Fig. 5b) are both in the intermediate region, and the O···O distance is considerably short (Tables 2 and 3). This hydrogen bond is intra-molecular, and there is no anionic network as shown in Fig. 5. Therefore, pyromellitate is a di-anion, and EDT-TTF is in a π-radical mono-cationic state. The geometry of EDT-TTF is consistent with this assignment as shown in Table 4. The EDT-TTF radical cations form a face-to-face stacked dimer, and these dimers form a mixed-stack column with the anions. There are also a few short S···O contacts.

β-[EDT-TTF$^+$]$_2$[(PMH$_2$)$^{2-}$] (5). This crystal is a polymorph of **4**. The *r* values and the features of the hydrogen bonds are almost the same, and there is no anionic network. Thus, pyromellitate is a di-anion, and EDT-TTF is in a π-radical mono-cationic state, though the geometry of EDT-TTF does not clearly indicate this state due to the poor quality of the crystal (Table 4). There are no short S···O contacts, while there are several short S···S contacts between the EDT-TTF radical cations. The EDT-TTFs form a co-planar 1-D chain via the S···S contacts along the *a* axis, as shown in Fig. 6b. The (PMH$_2$)$^{2-}$ planes are also co-planar to the EDT-TTF plane, which is parallel to the *ab* plane, and both (PMH$_2$)$^{2-}$ and EDT-TTF lie on a two-fold symmetry axis. As a result, the crystal is constructed of stacks of flat 2-D sheets composed of co-planar EDT-TTF and (PMH$_2$)$^{2-}$ (Fig. 6a). The inter-planar distance is rather short (about 3.3 Å), which is probably

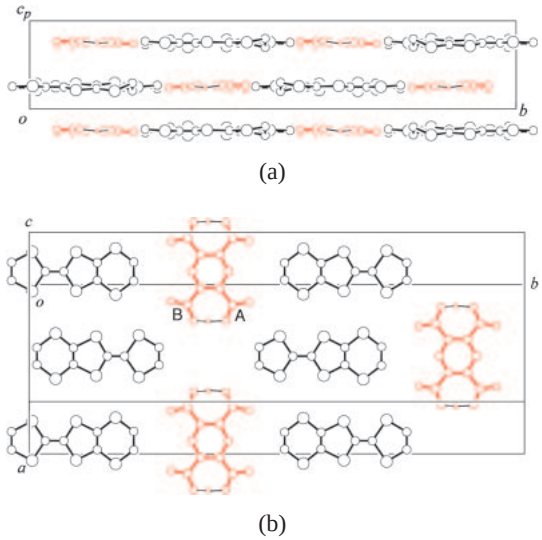

Fig. 6. Molecular arrangement in the EDT-TTF salt **5**. View parallel to the anionic plane (a) and view perpendicular to the anionic plane (b).

due to electrostatic interaction between the cations and anions.

[TMTSF$^+$]$_2$[(PMH$_2$)$^{2-}$](PMH$_4$)·2CH$_2$Cl$_2$ (6). In this crystal, there are two crystallographically independent (PMH$_{4-n}$)$^{n-}$ species, both of which are located at inversion centers. The *r* values of B and D (Fig. 7a) clearly indicate that they are carboxy groups, while those of A and C (Fig. 7a) are rather in the intermediate region. Since two protons in B and D participate in the hydrogen bonds with both of the oxygen atoms in A, A has been assigned as a carboxylato group. As a result, C has been assigned as a carboxy group because it forms a hydrogen bond with A. The real situation is, however, thought to be close to the intermediate hydrogen bond, in which one proton is shared by A and C, since the O···O distance between them is rather short (Table 3). In any case, the average number of deprotonation becomes 1, and each TMTSF is thus in a π-radical mono-cationic state from the composition. The geometry of TMTSF also supports this assignment (Table 4).

The (PMH$_{4-n}$)$^{n-}$ species form a 2-D network as shown in Fig. 7a. On the basis of hydrogen bond strength, the 1-D chain connected through A···C hydrogen bonds along the [101] direction is thought to dominate the (PMH$_{4-n}$)$^{n-}$ alignment, and then the 1-D chains are bound by A···B and A···D hydrogen bonds. The TMTSFs form a 1-D column between the sheets as shown in Fig. 7b. Each column is isolated by CH$_2$Cl$_2$ and the anionic sheets, and has two-fold periodicity.

General Remarks. (PMH$_2$)$^{2-}$ is known to form a 1-D chain (Fig. 1e) that has been frequently observed for mellitate with $n = 2$. However, such a 1-D network was not observed in the present system. The (PMH$_{4-n}$)$^{n-}$ species adopted 2-D (Figs. 1a and 1f for **1** and **3**, respectively) and 0-D (Fig. 1c for **4** and **5**) networks (excluding the H$_2$O bridged network in **2**). The constituents of the anionic network in **6** were somewhat similar to those in Fig. 1b; 1:1 mixture of $n = 0$ and $n = 2$ resulted in $n = 1$ in average. In contrast to the network in Fig. 1b, there were no intra-molecular hydrogen bonds in **6**. The network in **6** was a sort of modification of the rhombic-

type network as schematically shown in Fig. 8. In **6**, intra-molecular carboxy–carboxylato hydrogen bonds in the network in Fig. 1b were all replaced with inter-molecular ones between the $(PMH_2)^{2-}$ species. Therefore, the distance between the $(PMH_2)^{2-}$ species (shorter diagonal of the rhombus) was very short, resulting in shortening of the distance between the PMH_4 species. The resultant 2-D sheet was more condensed than the other 2-D sheets.

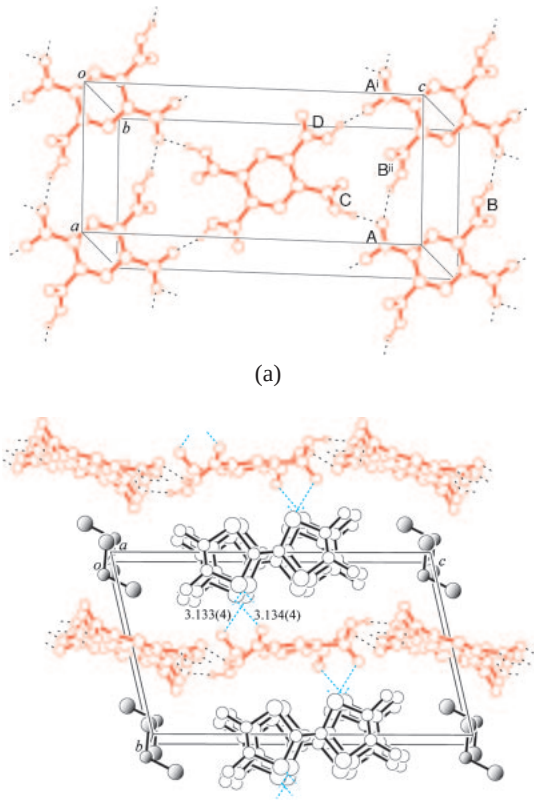

(a)

(b)

Fig. 7. Molecular arrangement in the TMTSF salt **6**. View perpendicular to the 2-D anionic sheet (a) and view parallel to both the sheet and the TMTSF column (b). Gray spheres are CH_2Cl_2. Hydrogen atoms not involved in hydrogen bonds are omitted.

The network structures in the present compounds were found to some extent to follow the correlation between networks and n, which has been observed in the ammonium salts of pyromellitate (Fig. 1). Compared with the ammonium cations so far studied, cations in the present system had no hydrogen-bonding ability. Therefore, the 2-D sheet networks should have been predominant in the present system.

pK_a of PMH_4 is slightly larger than that of mellitic acid. Thus, in some cases, pyridine derivatives were not strong enough deprotonating reagents to generate the $n = 2$ state. In such a case, method B was found to be effective to control n in the range of 1 and 2.

Method C was first designed to construct a network composed of two different benzenepolycarboxylato anions. Surprisingly, this method gave different products that could not be obtained by methods A and B, though the products did not contain any trimesic acid or its deprotonated anion. This observation strongly suggests that the crystal growth is kinetically rather than thermodynamically controlled, since the presence of different chemical species seriously affected the equilibrium state, which in turn affected the structure of the crystalline product. Though the details of the crystal-growth mechanism is not known, it is quite interesting that completely different crystals were obtained by adding a chemical species that could not be a component of the resultant crystal to the crystal growth solution.

In all the crystals studied, the TTF derivatives were all in a π-radical mono-cationic state. In addition, the cations were all dimerized except for **5**. These facts mean that the crystals were poor conductors with a non-magnetic ground state. Since the stabilization energy due to the dimerization of π-radicals was rather large (10–30 kJ mol^{-1}), the network of the $(PMH_{4-n})^{n-}$ species did not have enough strength to frustrate the dimer formation. In addition, all of the salts crystallized with stoichiometries that involved only mono-cationic spe-

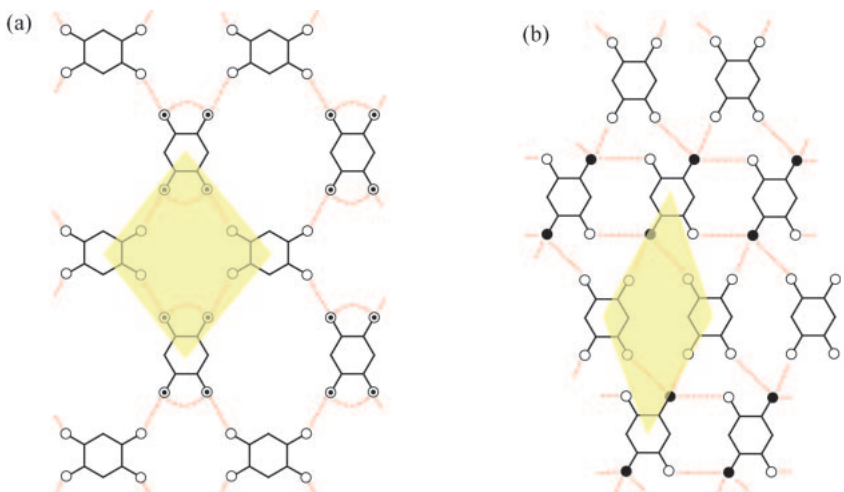

Fig. 8. Schematic representation of the 2-D anionic sheet of pyromellitate with $n = 0$ and 2. The extended Fig. 1b type sheet (a) and the sheet formed in **6** (b). Yellow region in (a) is a rhombic hole. The corresponding hole is much reduced in (b).

cies, and the extra space was filled by crystal solvents. These facts suggest that the relatively short S···O contacts govern the overall arrangement of the cations. This attractive interaction may prevent neutral donors from participating in the π–π interactions with the cationic portions in the crystal, namely, partially oxidized states of the donor assembly could not form.

Conclusion

In conclusion, this study showed that pyromellitic acid, which has two less carboxy groups than mellitic acid, also forms hydrogen-bonding networks when it is partially deprotonated, and that this anionic component can be utilized for the crystallization of π-radical cationic salts of the TTF derivatives. In contrast to mellitate, lack of carboxy/carboxylato groups at 3- and 6-positions in pyromellitate allowed for the formation of intra-molecular hydrogen bonds, leading to discrete di-anions in the crystal. However, in most of the cases, pyromellitate formed 2-D anionic networks mainly with a rhombic-type arrangement. The π-radical cations were packed between the anionic sheets, but the remaining extra space between the sheets was filled with crystal solvents. Attractive interactions between the cation and anion resulted in several short S···O contacts between them, which probably fixed the position and orientation of the cation.

From a comparison to the mellitate salts with the TTF derivatives, the dimensionality of the anionic networks was reduced in the pyromellitate salts. In the mellitate salts, the networks were 2-D and 3-D. The 2-D networks were constructed with infinite inter-anionic hydrogen bonds like pyromellitate, and the 3-D networks were stacked grids or laterally connected helical chains. The remaining space for the packing of cations was 2-D and 1-D, respectively. For pyromellitate, the maximum dimensionality of the anionic network seemed to be 2-D. Therefore, compared with mellitate, pyromellitate may be more advantageous to the design of systems with higher dimensionality in the cationic arrangement.

This work was supported in part by Grants-in-Aid for Scientific Research on Priority Areas of Molecular Conductors (No. 15073101) from the Ministry of Education, Culture, Sports, Science and Technology of the Japanese Government and Grants-in-Aid for Scientific Research (A) (No. 15205018) from the Japan Society for the Promotion of Science.

References

1 T. Inabe, *Bull. Chem. Soc. Jpn.* **2005**, *78*, 1373.
2 N. Kobayashi, T. Naito, T. Inabe, *Bull. Chem. Soc. Jpn.* **2003**, *76*, 1351.
3 N. Kobayashi, T. Naito, T. Inabe, *CrystEngComm* **2004**, *6*, 189.
4 N. Kobayashi, T. Naito, T. Inabe, *Adv. Mater.* **2004**, *16*, 1803.
5 T. Inabe, *J. Mater. Chem.* **2005**, *15*, 1317.
6 Y.-Q. Sun, J. Zhang, G.-Y. Yang, *Acta Crystallogr., Sect. E* **2002**, *58*, o1100.
7 S. H. Dale, M. R. J. Elsegood, M. Hemmings, A. L. Wilkinson, *CrystEngComm* **2004**, *6*, 207.
8 K. K. Arora, V. R. Pedireddi, *J. Org. Chem.* **2003**, *68*, 9177.
9 K. Biradha, M. J. Zaworotko, *Cryst. Eng.* **1998**, *1*, 67.
10 O. Felix, M. W. Hosseini, A. De Cian, *Solid State Sci.* **2001**, *3*, 789.
11 A. Altomare, M. C. Burla, M. Camalli, M. Cascarano, C. Giacovazzo, A. Guagliardi, G. Polidori, *J. Appl. Crystallogr.* **1994**, *27*, 435.
12 *SHELX97: Program for Crystal Structure Analysis*, G. M. Sheldrick, University of Göttingen, Germany, **1997**.
13 a) *CrystalStructure 3.5.1: Crystal Structure Analysis Package*, Rigaku and Rigaku/MSC, **2000–2003**. 9009 New Trails Dr., The Woodlands, TX 77381, U.S.A. b) *CRYSTALS Issue 10*, D. J. Watkin, C. K. Prout, J. R. Carruthers, P. W. Betteridge, Chemical Crystallography Laboratory, Oxford, UK, **1996**.
14 W. F. Cooper, N. C. Kenney, J. W. Edmonds, A. Nagel, F. Wudl, P. Coppens, *J. Chem. Soc., Chem. Commun.* **1971**, 889.
15 B. A. Scott, S. J. LaPlaca, J. B. Torrance, B. D. Silverman, B. Welber, *J. Am. Chem. Soc.* **1977**, *99*, 6631.
16 B. Garreau, D. De Montauzon, P. Cassoux, J.-P. Legros, J.-M. Fabre, K. Saoud, S. Chakroune, *New J. Chem.* **1995**, *19*, 161.
17 A. Hountas, A. Terzis, G. C. Papavassiliou, B. Hilti, J. Pfeiffer, *Acta Crystallogr., Sect. C: Cryst. Struct. Commun.* **1990**, *46*, 220.
18 T. J. Kistenmacher, T. J. Emge, P. Shu, D. O. Cowan, *Acta Crystallogr., Sect. B* **1979**, *35*, 772.
19 H. Kobayashi, A. Kobayashi, Y. Sasaki, G. Saito, H. Inokuchi, *Bull. Chem. Soc. Jpn.* **1983**, *56*, 2894.
20 S. Triki, L. Ouahab, J. Padiou, D. Grandjean, *J. Chem. Soc., Chem. Commun.* **1989**, 1068; S. Triki, L. Ouahab, J.-F. Halet, O. Peña, J. Padiou, D. Grandjean, C. Garrigou-Lagrange, P. Delhaes, *J. Chem. Soc., Dalton Trans.* **1992**, 1217.